Time-Dependent Solution of Three-Dimensional Compressible Turbulent Integral Boundary-Layer Equations

T. W. Swafford*
Sverdrup Technology Inc./AEDC Group, Arnold Air Force Station, Tennessee
and
D. L. Whitfield†
Mississippi State University, Mississippi State, Mississippi

An integral method is presented for computing three-dimensional, time-dependent, compressible, turbulent boundary layers in nonorthogonal curvilinear coordinates. Derivation of the momentum and mean-flow kinetic energy integral equations is given along with the auxiliary relations required for solution. Although the equations derived are valid for unsteady flow, only steady-state results are presented. The integral form of the equations is used in the interest of computational speed and because the three-dimensional method is an extension of an existing two-dimensional method. A time-dependent approach is used to provide a method that can use the same surface grid as an inviscid solver for use in viscous/inviscid interaction calculations. The equations are solved using a Runge-Kutta scheme with local time stepping to accelerate convergence. Stability and convergence of the numerical scheme are examined for various space difference approximations. Computed steady-state results are shown to compare favorably with measurements and with computations of previous investigators.

I. Introduction

THE coupling of an inviscid flow solver with a viscous flow solver has proved to be a useful method for the computation of viscous-inviscid interactive flow, particularly two-dimensional steady flow (see, e.g., Refs. 1-3). With the advancement of Euler equation codes capable of addressing three-dimensional flow,[4-7] the advancement of three-dimensional boundary-layer solution methods becomes important to handle practical three-dimensional problems. Providing adequate computational support to the testing mission at the Arnold Engineering Development Center (AEDC) requires reasonably accurate and inexpensive solutions of internal and external flows.[8] The application of a full Navier-Stokes code is expensive and time consuming, whereas a coupling approach can often provide an adequate flowfield solution at a much reduced cost. In this connection, the purpose of this paper is to present a new three-dimensional, time dependent, compressible, turbulent, integral boundary-layer computational method in nonorthogonal coordinates that can be used for transonic adiabatic flow. Although three-dimensional viscous-inviscid interaction is the ultimate goal, only the viscous (boundary-layer) portion of a coupling approach is addressed here.

The computation of three-dimensional boundary layers has received considerable attention in the past several years.[9-17] Typically, a calculation method is created to cater to a particular need and/or application. The following discussion addresses the requirement which led to the present approach.

The methods described in Refs. 9-17 can be classified as either integral or differential. In general, integral methods are computationally faster than differential methods because the former have one less space dimension to contend with. Although generally less flexible than differential methods, integral methods have often proved to be as accurate as differential methods for two-dimensional steady flow[18,19] because of the empiricism "built into" integral methods. Therefore, an integral approach is taken here in the interest of speed and accuracy and also because the three-dimensional method is an extension of an accurate two-dimensional method.[20] However, the question of accuracy between integral and differential methods for three-dimensional flow has been investi- ted to a much lesser degree than two-dimensional methc .[9,21,22]

When using a coupled approach, it is desirable that the viscous and inviscid surface grids (which could be nonorthogonal) be interchangeable such that information generated by one method can be conveyed back to the other easily. The steady form of the three-dimensional boundary-layer equations must be solved on a grid dictated by domain-of-dependence principles,[12,23] implying that interpolation is required on each viscous/inviscid iteration. However, if the time-dependent boundary-layer equations are used, the condition of interchangeable grids can be achieved because for a fixed grid system, an appropriate time step can be chosen to maintain computational stability. Thus, a time-dependent approach in nonorthogonal coordinates is adopted in order to provide a method than can use the same surface grid as an inviscid solver.

The system of equations used herein is the three-dimensional, time-dependent, compressible momentum and mean-flow kinetic energy integral equations. To take advantage of the previous work in two-dimensional flow, the nonorthogonal coordinates are related to streamline coordinates as suggested by Smith.[13] The streamwise and cross-flow velocity profiles used are those of Whitfield et al.[24] and Johnston,[25] respectively. The numerical scheme used and stability and convergence for various spatial difference approximations are discussed. Finally, computed steady-state results are compared with measurements and with computations of previous investigators.

Presented as Paper 83-1674 at the AIAA 16th Fluid and Plasma Dynamics Conference, Danvers, Mass., July 12-14, 1983; received July 30, 1983; revision received Oct. 1, 1984.

*Research Engineer, Computational Fluid Dynamics. Member AIAA.

†Professor, Department of Aerospace Engineering. Member AIAA.

II. Derivation of Equations

Inclusion of the derivation of the boundary-layer integral equations is important because these equations apparently do not exist in the literature for the general case of three-dimensional, time-dependent, compressible flow in nonorthogonal coordinates. Because of space limitations, only the major steps in arriving at the integral form of the equations are shown; more details are given in Ref. 26.

A. Differential to Integral Form

The starting point in deriving the integral form of the equations is to write the unsteady continuity and momentum boundary-layer equations in differential form as listed by Hirschel and Kordulla,[27] given here as

Continuity:

$$h_1h_2\sin\lambda\frac{\partial\rho}{\partial t}+\frac{\partial}{\partial x_1}(\rho u_1h_2\sin\lambda)+\frac{\partial}{\partial x_2}(\rho u_2h_1\sin\lambda)+\frac{\partial}{\partial x_3}(\rho u_3h_1h_2\sin\lambda)=0 \tag{1}$$

Momentum:

$$\rho h_1h_2\frac{\partial u_i}{\partial t}+\rho u_1h_2\frac{\partial u_i}{\partial x_1}+\rho u_2h_1\frac{\partial u_i}{\partial x_2}+\rho u_3h_1h_2\frac{\partial u_i}{\partial x_3}-\rho h_1h_2\cot\lambda K_iu_i^2+\rho h_1h_2\csc\lambda K_{3-i}u_{3-i}^2+\rho h_1h_2K_{i,3-i}u_1u_2=-h_{3-i}\csc^2\lambda\frac{\partial p}{\partial x_i}+h_i\cot\lambda\csc\lambda\frac{\partial p}{\partial x_{3-i}}+h_1h_2\frac{\partial\tau_{x_i}}{\partial x_3} \tag{2}$$

where $i=1$ or 2; i.e., when $i=1$, Eq. (2) is the x_1-momentum equation, and when $i=2$, Eq. (2) is the x_2-momentum equation. Note, however, that Eqs. (1) and (2) are not in the form shown in Ref. 27, but have been written instead using the nomenclature used, for example, by Cebeci et al.[16] where velocity and total stress components (u_i and τ_{x_i}, respectively) are the physical contravariant components with respect to the local nonorthogonal curvilinear coordinate system which is depicted in Fig. 1. In Eqs. (1) and (2), ρ and p are the fluid density and pressure, respectively, and λ the angle directed from the x_1 to the x_2 coordinate axis. Scale factors (h_i) and curvature terms (K_i,$K_{i,3-i}$) are listed by Cebeci et al.[16] and others.[26,27]

1. *Momentum Integral Equations*

The pressure gradient terms can be eliminated from Eq. (2) by: 1) multiplying by $\sin\lambda$ 2) writing this result at the edge of the layer, and then 3) subtracting this result from that of step 1. Manipulating the result of step 3 with the continuity equation [Eq. (1)] and assuming that $[\tau_{x_i}]_{\text{edge}}=0$, we get

$$\bar\rho h_1h_2\sin\lambda\frac{\partial\bar u_i}{\partial t}+\bar\rho h_2\sin\lambda\bar u_1\frac{\partial\bar u_i}{\partial x_1}+\bar\rho h_1\sin\lambda\bar u_2\frac{\partial\bar u_i}{\partial x_2}+\bar\rho\bar u_3h_1h_2\sin\lambda\frac{\partial\bar u_i}{\partial x_3}-\frac{\partial}{\partial t}(\rho u_ih_1h_2\sin\lambda)-\frac{\partial}{\partial x_1}(\rho u_iu_1h_2\sin\lambda)-\frac{\partial}{\partial x_2}(\rho u_2u_ih_1\sin\lambda)-\frac{\partial}{\partial x_3}(\rho u_3u_ih_1h_2\sin\lambda)-h_1h_2\cos\lambda K_i(\bar\rho\bar u_i^2-\rho u_i^2)+h_1h_2K_{3-i}(\bar\rho\bar u_{3-i}^2-\rho u_{3-i}^2)+h_1h_2\sin\lambda K_{i,3-i}(\bar\rho\bar u_1\bar u_2-\rho u_1u_2)+h_1h_2\sin\lambda\frac{\partial\tau_{x_i}}{\partial x_3}=0 \tag{3}$$

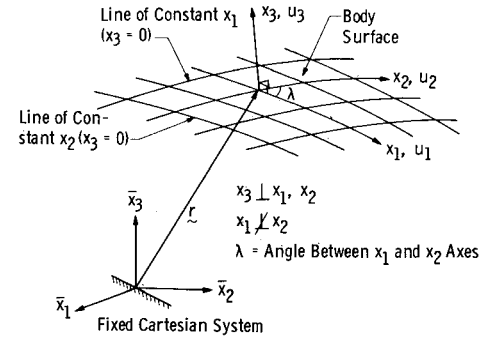

Fig. 1 General nonorthogonal curvilinear coordinate system on the body surface.

where overbars denote boundary-layer edge values. By taking $\partial\bar u_i/\partial x_3=0$, adding and substracting the term

$$\frac{\partial}{\partial t}(\rho\bar u_ih_1h_2\sin\lambda)+\frac{\partial}{\partial x_1}(\rho u_1\bar u_ih_2\sin\lambda)+\frac{\partial}{\partial x_2}(\rho u_2\bar u_ih_1\sin\lambda)+\frac{\partial}{\partial x_3}(\rho u_3\bar u_ih_1h_2\sin\lambda)$$

in Eq. (3) and using Eq. (1), considerable algebraic manipulation yields

$$h_1h_2\sin\lambda\left[\frac{\partial}{\partial t}(\bar\rho\bar u_i-\rho u_i)-\bar u_i\frac{\partial}{\partial t}(\bar\rho-\rho)\right]+h_2\sin\lambda(\bar\rho\bar u_1-\rho u_1)\frac{\partial\bar u_i}{\partial x_1}+h_1\sin\lambda(\bar\rho\bar u_2-\rho u_2)\frac{\partial\bar u_i}{\partial x_2}+\frac{\partial}{\partial x_1}[\rho u_1h_2\sin\lambda(\bar u_i-u_i)]+\frac{\partial}{\partial x_2}[\rho u_2h_1\sin\lambda(\bar u_i-u_i)]+\frac{\partial}{\partial x_3}[\rho u_3h_1h_2\sin\lambda(\bar u_i-u_i)]-h_1h_2\cos\lambda K_i[\bar u_i(\bar\rho\bar u_i-\rho u_i)+\rho u_i(\bar u_i-u_i)]+h_1h_2K_{3-i}[\bar u_{3-i}(\bar\rho\bar u_{3-i}-\rho u_{3-i})+\rho u_{3-i}(\bar u_{3-i}-u_{3-i})]+h_1h_2\sin\lambda K_{i,3-i}[\bar u_i(\bar\rho\bar u_{3-i}-\rho u_{3-i})+\rho u_{3-i}(\bar u_i-u_i)]+h_1h_2\sin\lambda\frac{\partial\tau_{x_i}}{\partial x_3}=0 \tag{4}$$

The x_1- and x_2-momentum integral equations are obtained by integrating Eq. (4) over $0\le x_3<\infty$. Using the assumption that surface metrics are independent of x_3,[28] defining the following integral thicknesses as

$$\bar\rho\bar q\delta_i^*=\int_0^\infty(\bar\rho\bar u_i-\rho u_i)\,dx_3,\quad \bar\rho\bar q^2\theta_{ij}=\int_0^\infty\rho u_j(\bar u_i-u_i)\,dx_3$$

$$\bar\rho\bar q^3\epsilon_{ij}=\int_0^\infty\rho u_j(\bar u_i^2-u_i^2)\,dx_3,\quad \bar q\delta_{u_i}^*=\int_0^\infty(\bar u_i-u_i)\,dx_3$$

$$\bar\rho\theta_\rho=\int_0^\infty(\bar\rho-\rho)\,dx_3 \tag{5}$$

and considering only an impermeable wall, i.e., $(\rho u_3)_{\text{wall}}=0$,

Eq. (4) becomes

$$\frac{1}{\bar{\rho}\bar{q}^2}\left[\frac{\partial}{\partial t}(\bar{\rho}\bar{q}\delta_i^*)-\bar{u}_i\frac{\partial}{\partial t}(\bar{\rho}\theta_\rho)\right]+\frac{1}{\bar{\rho}\bar{q}^2h_1h_2\sin\lambda}$$
$$\times\left[\frac{\partial}{\partial x_1}(\bar{\rho}\bar{q}^2h_2\sin\lambda\theta_{i1})+\frac{\partial}{\partial x_2}(\bar{\rho}\bar{q}^2h_1\sin\lambda\theta_{i2})\right]$$
$$+\frac{\delta_1^*}{h_1\bar{q}}\frac{\partial\bar{u}_i}{\partial x_1}+\frac{\delta_2^*}{h_2\bar{q}}\frac{\partial\bar{u}_i}{\partial x_2}-K_i\cot\lambda\left(\frac{\bar{u}_i}{\bar{q}}\delta_i^*+\theta_{ii}\right)$$
$$+K_{3-i}\csc\lambda\left(\frac{\bar{u}_{3-i}}{\bar{q}}\delta_{3-i}^*+\theta_{3-i,3-i}\right)$$
$$+K_{i,3-i}\left(\frac{\bar{u}_i}{\bar{q}}\delta_{3-i}^*+\theta_{i,3-i}\right)-\tfrac{1}{2}c_{f_{x_i}}=0 \qquad (6)$$

where $\bar{q}$ is the resultant velocity at the boundary-layer edge. The x_1- and x_2-momentum integral equations result from Eq. (6) by setting $i=1$ or 2, respectively. Also, a comma between subscripts such as $\theta_{i,3-i}$ is taken as θ_{12} for $i=1$ and θ_{21} for $i=2$.

2. Mean-Flow Kinetic Energy Integral Equation

The approach is to multiply Eq (3) by u_i, integrate over $0\le x_3<\infty$, and then sum the two resulting integral equations. Performing these operations and using Eq. (1) extensively results in

$$\bar{\rho}u_ih_1h_2\sin\lambda\frac{\partial\bar{u}_i}{\partial t}+\bar{\rho}\bar{u}_1u_ih_2\sin\lambda\frac{\partial\bar{u}_i}{\partial x_1}+\bar{\rho}\bar{u}_2u_ih_1\sin\lambda\frac{\partial\bar{u}_i}{\partial x_2}$$
$$+\bar{\rho}\bar{u}_3u_ih_1h_2\sin\lambda\frac{\partial\bar{u}_i}{\partial x_3}-\frac{1}{2}\left[\frac{\partial}{\partial t}(\rho u_i^2h_1h_2\sin\lambda)\right.$$
$$+\frac{\partial}{\partial x_1}(\rho u_1u_i^2h_2\sin\lambda)+\frac{\partial}{\partial x_2}(\rho u_2u_i^2h_1\sin\lambda)$$
$$\left.+\frac{\partial}{\partial x_3}(\rho u_3u_i^2h_1h_2\sin\lambda)\right]-h_1h_2\cos\lambda K_iu_i(\bar{\rho}\bar{u}_i^2-\rho u_i^2)$$
$$+h_1h_2K_{3-i}u_i(\bar{\rho}\bar{u}_{3-i}^2-\rho u_{3-i}^2)$$
$$+h_1h_2\sin\lambda K_{i,3-i}u_i(\bar{\rho}\bar{u}_1\bar{u}_2-\rho u_1u_2)+h_1h_2\sin\lambda u_i\frac{\partial\tau_{x_i}}{\partial x_3}=0 \qquad (7)$$

To Eq. (7), add and subtract the term

$$\frac{1}{2}\left[\frac{\partial}{\partial t}(\rho\bar{u}_i^2h_1h_2\sin\lambda)+\frac{\partial}{\partial x_1}(\rho u_1\bar{u}_i^2h_2\sin\lambda)\right.$$
$$\left.+\frac{\partial}{\partial x_2}(\rho u_2\bar{u}_i^2h_1\sin\lambda)+\frac{\partial}{\partial x_3}(\rho u_3\bar{u}_i^2h_1h_2\sin\lambda)\right]$$

and use the continuity equation and manipulate this result using the identities

$$\bar{\rho}u_i-\rho\bar{u}_i=\bar{u}_i(\bar{\rho}-\rho)-\bar{\rho}(\bar{u}_i-u_i)$$
$$\rho(\bar{u}_i^2-u_i^2)=\rho u_i(\bar{u}_i-u_i)+\bar{u}_i(\bar{\rho}\bar{u}_i-\rho u_i)-\bar{u}_i^2(\bar{\rho}-\rho)$$
$$\bar{\rho}\bar{u}_ju_i-\rho u_j\bar{u}_i=\bar{u}_i(\bar{\rho}\bar{u}_j-\rho u_j)-\bar{\rho}\bar{u}_j(\bar{u}_i-u_i)$$
$$u_i(\bar{\rho}\bar{u}_i^2-\rho u_i^2)=\rho u_i(\bar{u}_i^2-u_i^2)+\bar{u}_i^2(\bar{\rho}\bar{u}_i-\rho u_i)-\bar{\rho}\bar{u}_i^2(\bar{u}_i-u_i)$$
$$u_i(\bar{\rho}\bar{u}_{3-i}^2-\rho u_{3-i}^2)=\rho u_i(\bar{u}_{3-i}^2-u_{3-i}^2)+\bar{u}_{3-i}^2(\bar{\rho}\bar{u}_i-\rho u_i)$$
$$-\bar{\rho}\bar{u}_{3-i}^2(\bar{u}_i-u_i)$$
$$u_i(\bar{\rho}\bar{u}_i\bar{u}_j-\rho u_iu_j)=\rho u_j(\bar{u}_i^2-u_i^2)+\bar{u}_i^2(\bar{\rho}\bar{u}_j-\rho u_j)$$
$$-\bar{\rho}\bar{u}_i\bar{u}_j(\bar{u}_i-u_i),\qquad i\ne j \qquad (8)$$

Integrating over $0\le x_3<\infty$ using the integral thickness definitions given in Eq. (5), taking $\partial\bar{u}_i/\partial x_3=(\rho u_3)_{\text{wall}}=0$, and summing this result for $i=1$ and 2 yields the following clean but formidable equation:

$$\frac{1}{2\bar{\rho}\bar{q}^3}\frac{\partial}{\partial t}\left[\bar{\rho}\bar{q}^2(\theta_{11}+\theta_{22})+\bar{\rho}\bar{q}(\bar{u}_1\delta_1^*+\bar{u}_2\delta_2^*)-\bar{\rho}\theta_\rho(\bar{u}_1^2+\bar{u}_2^2)\right]$$
$$+\frac{1}{\bar{q}^2}\left(\frac{\bar{u}_1}{\bar{q}}\theta_\rho-\delta_{u_1}^*\right)\frac{\partial\bar{u}_1}{\partial t}+\frac{1}{\bar{q}^2}\left(\frac{\bar{u}_2}{\bar{q}}\theta_\rho-\delta_{u_2}^*\right)\frac{\partial\bar{u}_2}{\partial t}$$
$$+\frac{1}{2h_1h_2\sin\lambda\bar{\rho}\bar{q}^3}\left\{\frac{\partial}{\partial x_1}[h_2\sin\lambda\bar{\rho}\bar{q}^3(\epsilon_{11}+\epsilon_{21})]\right.$$
$$\left.+\frac{\partial}{\partial x_2}[h_1\sin\lambda\bar{\rho}\bar{q}^3(\epsilon_{12}+\epsilon_{22})]\right\}+\frac{\bar{u}_1}{h_1\bar{q}^2}(\delta_1^*-\delta_{u_1}^*)\frac{\partial\bar{u}_1}{\partial x_1}$$
$$+\frac{1}{h_1\bar{q}^2}(\bar{u}_2\delta_1^*-\bar{u}_1\delta_{u_2}^*)\frac{\partial\bar{u}_2}{\partial x_1}+\frac{1}{h_2\bar{q}^2}(\bar{u}_1\delta_2^*-\bar{u}_2\delta_{u_1}^*)\frac{\partial\bar{u}_1}{\partial x_2}$$
$$+\frac{\bar{u}_2}{h_2\bar{q}^2}(\delta_2^*-\delta_{u_2}^*)\frac{\partial\bar{u}_2}{\partial x_2}-K_1\cot\lambda\left[\epsilon_{11}+\frac{\bar{u}_1^2}{\bar{q}^2}(\delta_1^*-\delta_{u_1}^*)\right]$$
$$+K_2\csc\lambda\left[\epsilon_{21}+\frac{\bar{u}_2^2}{\bar{q}^2}(\delta_1^*-\delta_{u_1}^*)\right]$$
$$-K_2\cot\lambda\left[\epsilon_{22}+\frac{\bar{u}_2^2}{\bar{q}^2}(\delta_2^*-\delta_{u_2}^*)\right]$$
$$+K_1\csc\lambda\left[\epsilon_{12}+\frac{\bar{u}_1^2}{\bar{q}^2}(\delta_2^*-\delta_{u_2}^*)\right]$$
$$+K_{21}\left[\epsilon_{21}+\frac{\bar{u}_2}{\bar{q}^2}(\bar{u}_2\delta_1^*-\bar{u}_1\delta_{u_2}^*)\right]$$
$$+K_{12}\left[\epsilon_{12}+\frac{\bar{u}_1}{\bar{q}^2}(\bar{u}_1\delta_2^*-\bar{u}_2\delta_{u_1}^*)\right]$$
$$+\frac{1}{\bar{\rho}\bar{q}^3}\int_0^\infty\left(u_1\frac{\partial\tau_{x_1}}{\partial x_3}+u_2\frac{\partial\tau_{x_2}}{\partial x_3}\right)dx_3=0 \qquad (9)$$

Therefore, in summary: 1) the momentum integral equations are given by Eq. (6) for $i=1$ and 2, 2) the mean-flow kinetic energy integral equation is given by Eq. (9), and 3) the integral lengths are given by Eq. (5).

However, further algebraic manipulation is required to put these equations in a form amenable to solution. Equations (6) and (9) can be written as

$$\frac{1}{\bar{\rho}\bar{q}^2}\left[\frac{\partial}{\partial t}(\bar{\rho}\bar{q}\delta_i^*)-\bar{u}_i\frac{\partial}{\partial t}(\bar{\rho}\theta_\rho)\right]=\ell_i,\qquad i=1\text{ or }2 \qquad (10)$$

$$\frac{1}{2\bar{\rho}\bar{q}^3}\frac{\partial}{\partial t}[\bar{\rho}\bar{q}^2(\theta_{11}+\theta_{22})+\bar{\rho}\bar{q}(\bar{u}_1\delta_1^*+\bar{u}_2\delta_2^*)-\bar{\rho}\theta_\rho(\bar{u}_1^2+\bar{u}_2^2)]$$
$$+\frac{1}{\bar{q}^2}\left[\left(\frac{\bar{u}_1}{\bar{q}}\theta_\rho-\delta_{u_1}^*\right)\frac{\partial\bar{u}_1}{\partial t}+\left(\frac{\bar{u}_2}{\bar{q}}\theta_\rho-\delta_{u_2}^*\right)\frac{\partial\bar{u}_2}{\partial t}\right]=L \qquad (11)$$

where ℓ_i and L are defined by referring to Eqs. (6) and (9).

Expanding the derivatives with respect to time results in (for $i=1$ and 2)

$$\frac{\partial\delta_1^*}{\partial t}-\frac{\bar{u}_1}{\bar{q}}\frac{\partial\theta_\rho}{\partial t}=\bar{q}\ell_1-T_{\ell_1} \qquad (12)$$

$$\frac{\partial}{\partial t}(\theta_{11}+\theta_{22})=2\bar{q}L-T_L-\frac{\bar{u}_1}{\bar{q}}(\bar{q}\ell_1-T_{\ell_1})-\frac{\bar{u}_2}{\bar{q}}(\bar{q}\ell_2-T_{\ell_2}) \qquad (13)$$

$$\frac{\partial\delta_2^*}{\partial t}-\frac{\bar{u}_2}{\bar{q}}\frac{\partial\theta_\rho}{\partial t}=\bar{q}\ell_2-T_{\ell_2} \qquad (14)$$

where T_{ℓ_1}, T_{ℓ_2}, and T_L are terms involving the time rate of change of $\bar{\rho}$, $\bar{u}_i$, and $\bar{q}$. Up to this point, the equations are valid for time-varying edge conditions. It is to be emphasized that, hereafter, the analysis is restricted to the case of steady edge conditions, i.e., $T_{\ell_i} = T_L = 0$. Thus, the system of equations reduces to

$$\frac{\partial \delta_1^*}{\partial t} - \frac{\bar{u}_1}{\bar{q}} \frac{\partial \theta_\rho}{\partial t} = \bar{q}\ell_1 \tag{15}$$

$$\frac{\partial}{\partial t}(\theta_{11} + \theta_{22}) = 2\bar{q}L - \bar{u}_1\ell_1 - \bar{u}_2\ell_2 \tag{16}$$

$$\frac{\partial \delta_2^*}{\partial t} - \frac{\bar{u}_2}{\bar{q}} \frac{\partial \theta_\rho}{\partial t} = \bar{q}\ell_2 \tag{17}$$

Equations (15-17) contain the 13 unknowns δ_i^*, θ_{ij}, ϵ_{ij}, $\delta_{u_i}^*$, and θ_ρ ($i = 1$ or 2 and $j = 1$ or 2). The fundamental steps in reducing the number of unknowns to three in the present analysis are 1) the choice of the cross-flow velocity profile, 2) relating the 13 integral lengths in streamline coordinates such that specification of Δ_1^*, Θ_{11}, E_{11}, θ_ρ, and Δ_u^* completely determines the rest, 3) relating the nonorthogonal integral lengths to those in streamline coordinates, and 4) the choice of shape factor and skin-friction correlations in streamline coordinates. The following sections address the manner in which these tasks are resolved. It should be noted that integral lengths written with upper-case Greek letters represent those in streamline coordinates, whereas lower-case letters denote integral lengths resolved in the nonorthogonal system.

B. Empirical Relationships in Streamline Coordinates

1. Cross-Flow Velocity Profile

The choice of cross-flow velocity profile is restricted in the present study to the triangular model of Johnston,[25] given as

$$u_n/u_s = \tan(\beta_w) \tag{18}$$

in the thin layer adjacent to the wall, and over the remaining portion of the boundary layer

$$u_n/\bar{q} = A[1 - (u_s/\bar{q})] \tag{19}$$

where u_s and u_n are streamwise and cross-flow velocity components, respectively, and A is a parameter related to the limiting wall streamline angle β_w. In the present case, the relationship originally given by Johnston[25] and later modified by Smith[13] as

$$\tan(\beta_w) = A\left\{\frac{0.1}{[c_f \cos(\beta_w)(1 + 0.18M_e^2)]^{1/2}} - 1\right\} \tag{20}$$

is used, where c_f is the value of skin friction resolved along the external streamline flow direction.

2. Shape Factor, Skin-Friction, and Dissipation Correlations

The following shape factors can be defined in streamline coordinates as

$$H = \frac{\Delta_1^*}{\Theta_{11}}, \quad H_{\theta_\rho} = \frac{\theta_\rho}{\Theta_{11}}, \quad H_{\theta^*} = \frac{E_{11}}{\Theta_{11}}, \quad \frac{\Theta_{11}}{\Theta_u}, \quad \bar{H} = \frac{\Delta_u^*}{\Theta_u} \tag{21}$$

(See Refs. 13 and 26 for the definitions of streamwise integral thicknesses.) Based upon the streamwise velocity profile originally postulated by Whitfield[29] and a velocity-temperature relationship derived by Whitfield and High,[30] it was shown in Ref. 20 that H, Θ_{11}/Θ_u, and H_{θ^*} can be correlated with $\bar{H}$ and edge Mach number M_e. In addition, Donegan[31] correlated H_{θ_ρ} with $\bar{H}$ and M_e, listed here as

$$H_{\theta_\rho} = M_e^2(0.185\bar{H} + 0.150) \tag{22}$$

The correlations for H_{θ^*} and c_f actually used in the present study are given by Whitfield et al.[32] The H_{θ^*} correlation is based upon a streamwise velocity profile valid for attached and separated flow.[24,33] These correlations are used because of their validity over a larger range of $\bar{H}$ than those given in Ref. 20.

The equations used to resolve c_f in streamwise coordinates into nonorthogonal components are those of Myring[12] and Smith.[13]

$$c_{f_{x_1}} = c_f\left[\frac{\sin(\xi) - \cos(\xi)\tan(\beta_w)}{\sin(\lambda)}\right]$$

$$c_{f_{x_2}} = c_f\left[\frac{\sin(\alpha) + \cos(\alpha)\tan(\beta_w)}{\sin(\lambda)}\right] \tag{23}$$

where α is the angle between the local edge resultant velocity vector and the x_1 axis, λ the angle between the x_1 and x_2 axes, and $\xi \equiv \lambda - \alpha$.

Finally, the dissipation integrals appearing in Eq. (9) can be written in terms of streamwise and cross-flow velocities and then integrated by parts using Johnston's cross-flow profile, yielding

$$\frac{1}{\bar{\rho}\bar{q}^3}\int_0^\infty \left(u_1 \frac{\partial \tau_{x_1}}{\partial x_3} + u_2 \frac{\partial \tau_{x_2}}{\partial x_3}\right) dx_3 = -\frac{1}{\sin^2\lambda}\frac{c_f D_u^s}{2}\left(t_1 + t_2 \frac{D_u^n}{D_u^s}\right) \tag{24}$$

where

$$D_u^s = \int_0^\infty \frac{\tau_s}{\tau_{s_w}} \frac{\partial(u_s/\bar{q})}{\partial x_3} dx_3 \tag{25}$$

$$D_u^n = \int_0^\infty \tan\beta \frac{\tau_s}{\tau_{s_w}} \frac{\partial(u_s/\bar{q})}{\partial x_3} dx_3 \tag{26}$$

and t_1 and t_2 are functions of ξ, α, and A.[26] The "streamwise" dissipation (D_u^s) is evaluated in this study using the correlation developed by Donegan[31] and later improved by Thomas.[34] (The product $c_f D_u^s/2$ was actually correlated as a function of $\bar{H}$, M_e, and $Re_{\Theta_{11}}$.) This correlation was derived by numerically evaluating Eq. (25) using a constant laminar plus turbulent shear stress in the region very near the wall, an eddy-viscosity model in the inner and outer regions, and the derivative of the velocity profile used in Ref. 24. In principle, the "cross-flow" dissipation D_u^n could be correlated in similar fashion using Johnston's cross-flow profile to evaluate $\tan\beta$. However, we have opted here to simply neglect the contribution of D_u^n in comparison with D_u^s with the understanding that this approximation could lead to serious error for flows containing "large" cross flow.

C. Relationships Between Streamwise and Nonorthogonal Integral Lengths Using Johnston's Cross-Flow Profile

Using Johnston's cross-flow profile in the streamwise integral lengths defined in Ref. 13 and shape factors defined in Eq. (21), the following relations among streamline integral

lengths can be derived:

$$\Theta_{21} = -A\Theta_{11} \qquad E_{12} = \Theta_{12} + \Theta_{21}(H_{\theta^*} - 2)$$

$$\Delta_2^* = \Theta_{21}(H - H_{\theta_\rho}) \qquad E_{21} = -\Theta_{22} - AE_{12}$$

$$\Theta_{12} = \Theta_{21} - \Delta_2^* \qquad E_{22} = -A(E_{21} - \Theta_{22})$$

$$\Theta_{22} = -A\Theta_{12} \qquad \Delta_v^* = -A\Delta_u^* \tag{27}$$

(These relationships were derived using only the outer portion of Johnston's model.) Therefore, given Θ_{11}, $\bar{H}$, A, H, H_{θ_ρ}, H_{θ^*}, and Θ_{11}/Θ_u, all streamwise integral quantities can be determined. As mentioned previously, H, H_{θ_ρ}, H_{θ^*} and Θ_{11}/Θ_u are related to $\bar{H}$ and M_e.[20,31,32] Smith[13] points out that all integral quantities in one axis system are uniquely related to those in the other. (These relations are independent of the cross-flow velocity profile.) For example, Smith shows that the momentum thickness θ_{11} in the nonorthogonal system is related to those in the streamline system as

$$\theta_{11} = \frac{1}{\sin^2\lambda}[\Theta_{11}\sin^2\xi - (\Theta_{12} + \Theta_{21})\sin\xi\cos\xi + \Theta_{22}\cos^2\xi] \tag{28}$$

Stock[14] has listed all of these relationships using different nomenclature than used herein, whereas Myring[12] and Smith[13] have given the relationships between streamline and nonorthogonal displacement and momentum thicknesses. The complete list using the present nomenclature is given in Ref. 26.

Therefore, given the external Mach number as input, the only remaining unknowns are Θ_{11}, $\bar{H}$, and A; it remains to reformulate the system of Eqs. (15-17) in terms of these quantities.

D. Formulation for Solution

Using the relations between streamline and nonorthogonal integral lengths given in Ref. 26, the aforementioned empirical correlations, and assuming steady edge conditions, Eqs. (15-17) can be recast into matrix form as

$$\hat{A}\frac{\partial}{\partial t}(U) = b \tag{29}$$

where $\hat{A}$ is the 3×3 coefficient matrix; U the vector of unknowns, $=(\Theta_{11},\bar{H},A)^T$; and b the right-hand side vector containing spatial derivatives; and the elements of the matrix $\hat{A}$ and vector b are given in Ref. 26. Equation (29) represents a system of three first-order, nonlinear, coupled partial differential equations (pde) for the three unknowns, Θ_{11}, $\bar{H}$, and A. The numerical approach taken here is, first, to reduce the above system of pde's to a system of ordinary differential equations (ode) by discretizing the dependent variables in space and then using a standard integrator for ode's. Particular aspects of the numerical method used herein are discussed in the following section.

III. Numerical Method

The aforementioned numerical appoach is usually referred to as the method of lines. Recently, Jameson et al.[35] used this method to solve the Euler equations in transonic flow and showed that when using a Runge-Kutta scheme, convergence to steady state was significantly accelerated by using a local time step dictated by the local CFL number. The approach taken here is a four-stage Runge-Kutta scheme also using spatially variable time steps to accelerate convergence. (One should recall from the latter part of Sec. II.A.2 that because edge condition derivatives were set to zero, only steady-state results are of interest. Hence transient results were not considered important for the present work.)

A. Implementing Four-Stage Runge-Kutta

Consider the single model equation

$$\frac{\partial u}{\partial t} + a\frac{\partial u}{\partial x} = 0, \qquad a = \text{const} > 0 \tag{30}$$

applied in the x-t plane. By expressing the spatial derivative with some appropriate finite difference approximation to be discussed later, Eq. (30) becomes

$$\frac{du_i}{dt} = -aD_x(u_i^n) \equiv f(t,u_i^n) \tag{31}$$

where $D_x(u_i^n)$ is some finite difference operator and u_i^n denotes the ith value of u at time level n. For the case of two space dimensions, Eq. (31) becomes

$$\frac{du_{ij}}{dt} = -aD_{x_1}(u_{ij}^n) - bD_{x_2}(u_{ij}^n) \tag{32}$$

with corresponding changes in Eq. (31) for $f(t,u_i^n)$. For the present system of equations, Eq. (29) can be written as

$$\frac{dU_{ij}}{dt} = -\hat{a}D_{x_1}(U_{ij}^n) - \hat{b}D_{x_2}(U_{ij}^n) + c \tag{33}$$

where U_{ij} is the vector of unknowns and $\hat{a}$ and $\hat{b}$ are 3×3 matrices. Thus, if we write Eq. (33) at every (i,j) point in the field, the solution can be advanced from time level n to time level $n+1$ using a standard Runge-Kutta scheme.[36]

B. Stability and Convergence

Although a system of equations is involved, the numerical method described above is explicit. Typically, stable explicit methods are restricted to CFL numbers less than one. However, Jameson et al.[35] showed that, for the model problem Eq. (30) using central space differences, the "classical"

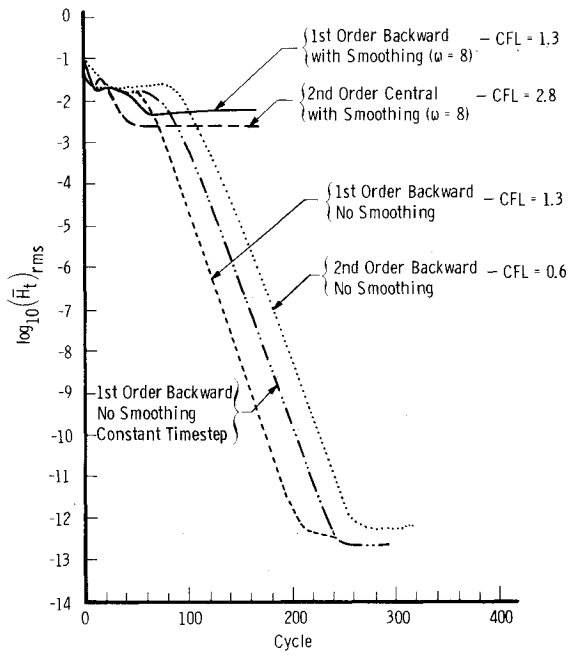

Fig. 2 Convergence histories for the dummy infinite swept-wing test case of Cumpsty and Head.[15]

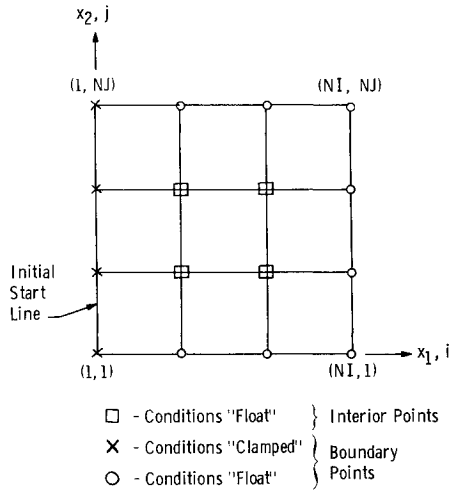

Fig. 3 General computational domain.

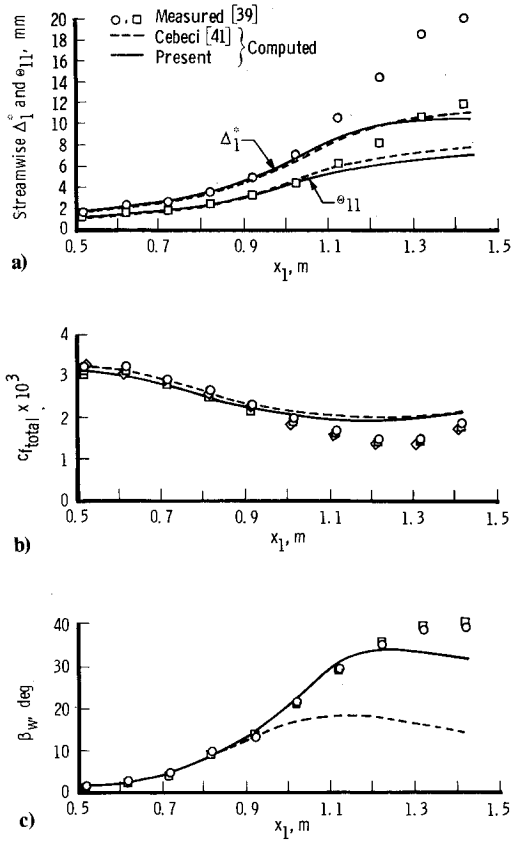

Fig. 4 Computed and measured boundary-layer quantities for the van den Berg and Elsenaar[39] infinite swept-wing case. a) Displacement and momentum thickness; b) total skin friction; c) wall streamline angle.

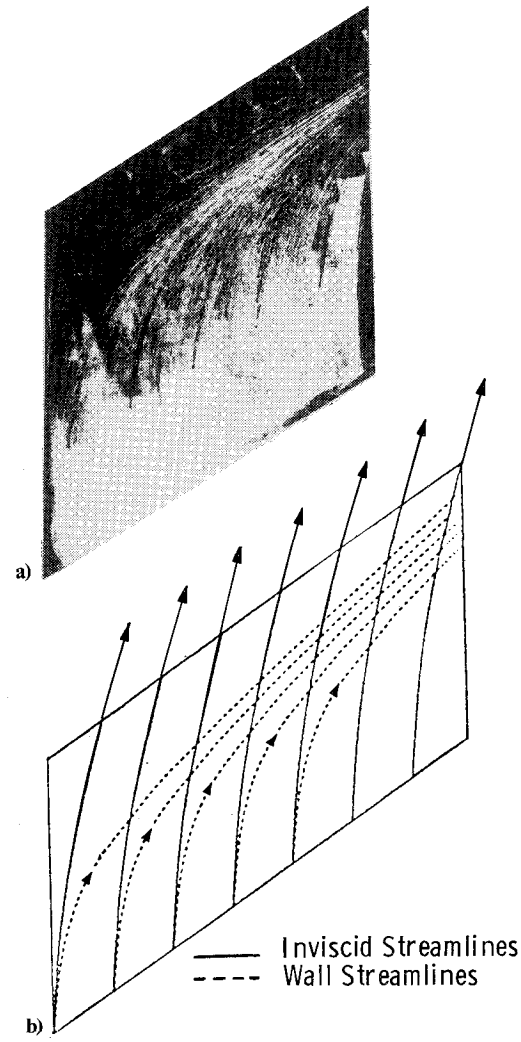

Fig. 5 Computed and measured wall streamlines for the van den Berg and Elsenaar[39] test case: a) measured (oil-flow photograph); b) computed wall streamlines.

Runge-Kutta scheme[36] was stable for CFL numbers $<2\sqrt{2}$. Initially, the present system of equations was solved using central space differences with a CFL = 2.8. Smoothing was required and, although reasonable answers were obtained, convergence was not good and the amount of smoothing needed was problem dependent. After examining the eigenvalues of the $\hat{a}$ and $\hat{b}$ matrices in Eq. (33), it was found that, for most cases considered, eigenvalues for both the $\hat{a}$ and $\hat{b}$ matrices were positive. As shown by Steger and Warming[37] a stable scheme for the model problem can be constructed using backward space differences which has better dissipative and dispersion properties than that of a centered scheme, thus requiring little or no smoothing. However, using backward space differences necessitates reducing the maximum allowable CFL number from 2.8 to approximately 1.3 and 0.6 for first- and second-order backward differences, respectively, to maintain stability.[26]

Figure 2 illustrates convergence obtained (as measured by the rms of the $\partial\bar{H}/\partial t$ derivative) for the dummy infinite swept wing test case of Cumpsty and Head[15] solving the present system using second-order central/first-order, backward, and second-order backward spatial differences with a spatially variable time step. A simple five-point weighted-average smoothing was employed to obtain the solution using central differences with smoothing. Also shown in Fig. 2 is the convergence history of the first-order backward scheme with smoothing, which illustrates that convergence is limited when smoothing is applied. In addition, Fig. 2 illustrates how convergence is accelerated by using spatially variable time steps as opposed to using a constant (maximum allowable over the field) time step.

Solutions presented herein were converged such that all residuals were reduced to machine zero [$\Theta(10^{-14})$] on a CRAY-1S. Typical run times were approximately 0.001 CPU seconds/cycle/point using a four-stage Runge-Kutta scheme. Depending upon the time step used, 200-400 cycles were required for convergence. The above rather stringent convergence criteria were used because the present code is in a

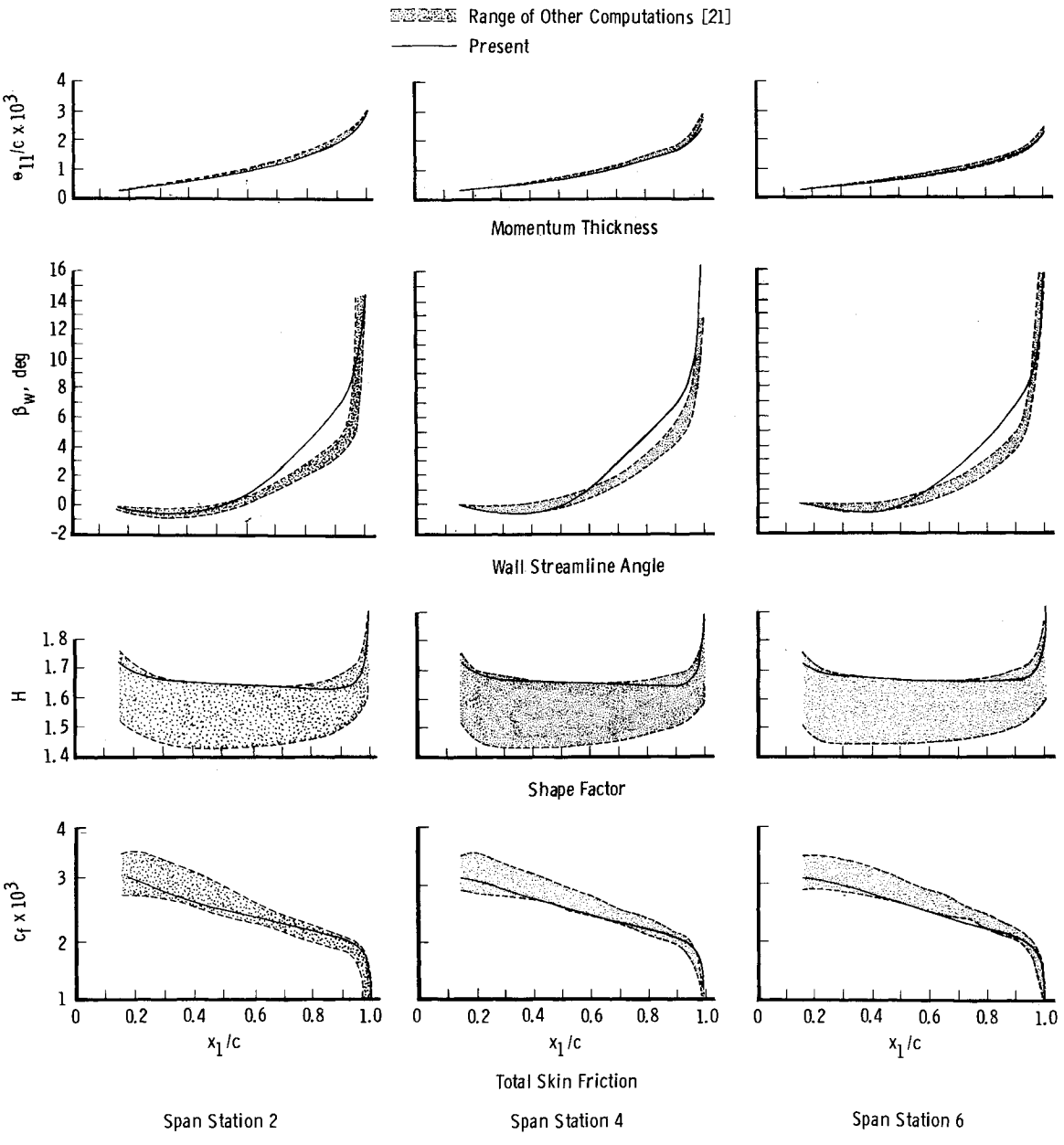

Fig. 6 Calculated boundary-layer parameters for the 1978 Stockholm test case[21] for zero angle of attack.

research stage; however, for practical applications, adequate solutions can be obtained by reducing the residuals only three or four orders of magnitude. The overall speed of the present integral method is somewhat slow considering that speed and simplicity were the reasons that an integral method was chosen in the first place. However, as mentioned above, the present code is not for production runs and its performance could be improved significantly by more efficient coding and by the incorporation of a more efficient numerical scheme. For example, a two-stage Runge-Kutta scheme operating with a CFL of 0.9 was incorporated into the code and the van den Berg case (to be discussed in Sec. V) recomputed. The solution was practically identical to that using the four-stage scheme with approximately a 40% reduction in CPU time.

C. Boundary Conditions

Depicted in Fig. 3 is a general computational mesh as used in the present method. The boundary conditions used to compute all of the solutions presented here were to fix or "clamp" the three dependent variables (Θ_{11}, $\bar{H}$, and A) along the initial start line (say, along the leading edge of a wing) and let the conditions at all other boundaries "float." That is, no conditions along any boundary except the initial start line were specified. This essentially amounts to extrapolating the conditions at the boundaries from the interior of the computational domain.

As previously mentioned, all eigenvalues of both the $\hat{a}$ and $\hat{b}$ matrices in Eq. (33) for most flow cases are positive. Therefore, specification of boundary conditions along the initial start line ($I=1$, $J=1\rightarrow NJ$) and extrapolation along the "outflow" boundary ($I=NI$, $J=1\rightarrow NJ$) is compatible with the sign of the characteristics (eigenvalues). However, the sign of the eigenvalues of the $\hat{b}$ matrix are mixed for some flow cases. Therefore, extrapolation of boundary conditions along the ($I=1\rightarrow NI$, $J=1$) line and ($I=1\rightarrow NI$, $J=NJ$) line is not correct if one adheres strictly to the information obtained from the sign of the eigenvalues. However, based upon the results to be presented, it seems that this erroneous treatment of conditions along the upper and lower boundaries does not affect the outcome of the computations sig-

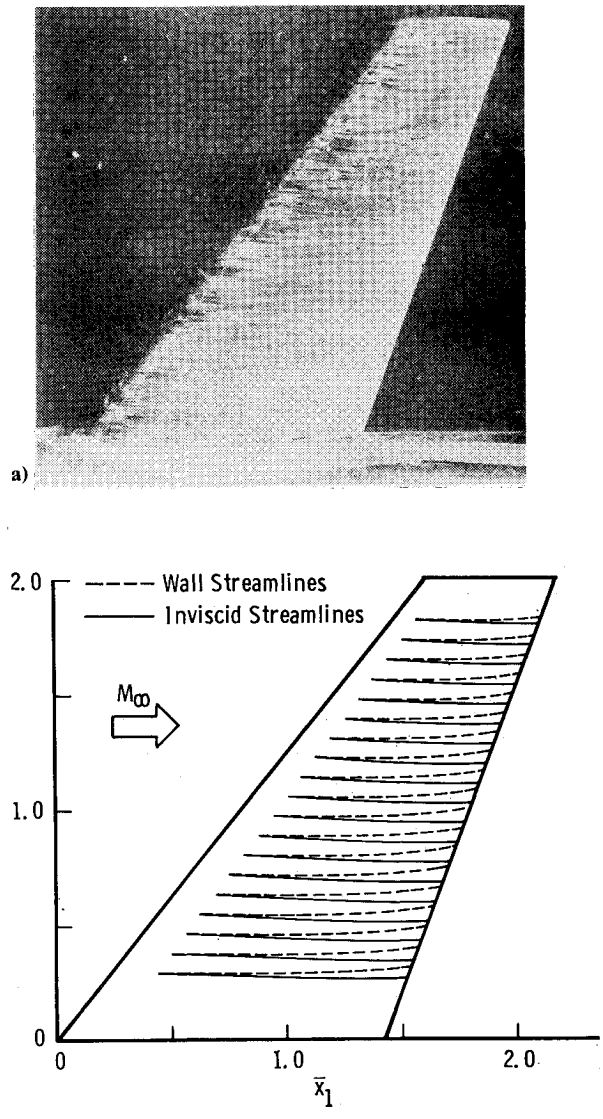

Fig. 7 Computed and measured streamline patterns for the 1978 Stockholm test case[21] for zero angle of attack: a) measured (surface-flow visualization); b) computed.

nificantly, at least for the cases considered. It should be noted that initial conditions for all cases were taken as those at the initial start line (for each case) distributed over the entire mesh. Different initial conditions were tested which did not alter the steady-state solutions.

IV. Computation of Surface Metrics

The primary objective of the present work was to develop a three-dimensional, time-dependent, turbulent boundary-layer computational method that can be used for compressible adiabatic flow in nonorthogonal coordinates. All but one of the cases computed thus far were such that specification of surface scale factors and curvatures was trivial (i.e., $h_1=h_2=1$ and $K_1=K_2=K_{12}=K_{21}=0$); only one case was computed using surface metrics which themselves were computed from the given Cartesian coordinates of the surface.

As shown by Smith and Gaffney,[38] all metrics depend explicitly upon derivatives of the given Cartesian coordinates with respect to the chosen curvilinear coordinates. For one test case, these derivatives were evaluated using simple central differences except near the boundaries where extrapolation was used. This is a rather crude approximation compared to, for example, the method described by Smith and Gaffney,[38] who approximated the metric tensor using bicubic splines. However, computed results indicate that the approximation used here was adequate for the case considered, which was a flat surface using a skewed grid (i.e., a swept finite wing with taper). It is not known what effects a more accurate calculation of surface metrics would have on the solution.

V. Results

Calculations using the present method are compared with results of two experimental/analytical test cases. These data sets include the infinite swept wing case of van den Berg and Elsenaar[39] and the fully three-dimensional case of Humphreys.[21] Additional comparisons can be found in Refs. 26 and 40.

The low-speed flow used by van den Berg and Elsenaar[39] involved probing the three-dimensional boundary layer on a flat surface swept at 35 deg with an external pressure distribution induced by an appropriately shaped body such that infinite swept-wing conditions were approximately simulated. (This experiment was performed specifically for comparison to computational methods.) Comparisons between measured and computed boundary-layer quantities are shown in Fig. 4. Agreement between the computations and measurements upstream of $x=1$ m is considered good; whereas, past this point, considerable discrepancies exist, particularly with the streamwise integral thicknesses. Similar results were obtained by Cebeci and Chang[41] using a finite difference method. However, the measured flow angles downstream of $x=1$ deviated from those which would have been present under infinite swept-wing conditions.[39] Illustrated in Fig. 5 are computed and measured wall streamlines which indicate good qualitative agreement of the experiment and computations.

The 1978 Stockholm test case[21] was based upon the flow about a swept wing of modern configuration in high subsonic flow ($M=0.5$). Effects of three dimensionality and compressibility were small but non-negligible. Because the test case was designed to test three-dimensional boundary-layer calculation methods, the inviscid velocity distribution was provided by a higher order panel method. The only experimental data provided for comparison were oil-flow photographs of the wing surface. Boundary values at the initial start line are given in Ref. 21. Figure 6 gives comparisons between the results at span stations 2, 4, and 6 computed by the present method and the eight calculation methods (represented by the shaded area in Fig. 6) which were compared in Ref. 21 for the case of zero angle of attack. Favorable agreement is seen to exist when comparing momentum thickness, shape factor, and skin fricition; whereas, the present computations for β_w indicate a more rapid increase for $x/c>0.4$ than the other calculations. Figure 7 gives the wall streamline patterns as computed by the present method and as measured using oil-flow visualization; good qualitative agreement is seen to exist between the computations and measurements.

VI. Summary and Conclusions

An integral method for computing three-dimensional, time-dependent, compressible, turbulent boundary layers in nonorthogonal coordinates has been presented. A derivation of the time-dependent momentum and mean-flow kinetic energy integral equations was presented and the resulting method provides a means for viscous/inviscid interaction using identical surface grids for both the viscous and inviscid calculations. A four-stage, Runge-Kutta, time-stepping scheme was used to numerically solve the system of equations using local time steps to accelerate convergence. Several space difference approximations were employed, and it was found that a backward scheme gave the best results using no artificial smoothing. Calculated results using the present method were compared to experimental data and the results

of other calculation methods and satisfactory agreement was obtained. However, it is felt that results can be improved by incorporating more general correlations pertaining to three-dimensional boundary-layer flow, particularly an improved cross-flow velocity profile representation. The Stockholm swept-wing calculation demonstrates that three-dimensional turbulent boundary-layers can be computed in a time-dependent fashion on a practical configuration using the present method.

Acknowledgments

The work reported herein was conducted by the Arnold Engineering Development Center (AEDC), Air Force Systems Command (AFSC). Work and analysis for this research were done by personnel of Sverdrup Technology Inc./AEDC Group, operating contractor for the AEDC propulsion test facilities. Further reproduction is authorized to satisfy needs of the U.S. Government.

References

[1]Lock, R. C., "A Review of Methods for Predicting Viscous Effects on Aerofoils and Wings at Transonic Speed," AGARD-CPP-291, 1980.

[2]Melnik, R. E., "Turbulent Interactions on Airfoils at Transonic Speeds—Recent Developments," AGARD-CPP-291, 1980.

[3]Le Balleur, J. C., "Viscid-Inviscid Coupling Calculations for Two and Three Dimensional Flows," Lecture Series 1982-04, von Kármán Institute for Fluid Dynamics, March-April 1982.

[4]Jacocks, J. L. and Kneile, K. R., "Computation of Three-Dimensional Time-Dependent Flow Using the Euler Equations," AEDC-TR-80-99 (AD-A102463), Oct. 1980.

[5]Rizzi, A. and Erickson, L. E., "Transfinite Mesh Generation and Damped Euler Equation Algorithm for Transonic Flow Around Wing-Body Configurations," AIAA Paper 81-0999, June 1981.

[6]Schmidt, W., Jameson, A., and Whitfield, D., "Finite Volume Solutions to the Euler Equations in Transonic Flow," *Journal of Aircraft*, Vol. 20, Feb. 1983, pp. 127-133.

[7]Whitfield, D. and Jameson, A., "Three-Dimensional Euler Equation Simulation of Propeller-Wing Interaction in Transonic Flow," AIAA Paper 83-0236, Jan. 1983.

[8]Barton, J. M., "The Role of CFD in Aeropropulsion Ground Testing," AIAA Paper 83-0149, Jan. 1983.

[9]East, L. R., "Computation of Three Dimensional Turbulent Boundary Layers," Euromech 60, Trondheim, AFA TN AE-1211, 1975.

[10]Wesseling, P. and Lindhout, J. P. F., "A Calculation Method for Three-Dimensional Incompressible Turbulent Boundary Layers," *Turbulent Shear Flows*, AGARD Conference Proceedings, No. 73, Paper 8, 1971.

[11]Lindhout, J. P. F., Moek, G., de Boer, E., and van den Berg, B., "A Method for the Calculation of 3D Boundary Layers on Practical Wing Configurations," ASME Conference on Turbulent Boundary Layers, Niagara Falls, N.Y., 1979.

[12]Myring, D. F., "An Integral Prediction Method for Three-Dimensional Turbulent Boundary Layers in Incompressible Flow," RAE TR-70147, Aug. 1970.

[13]Smith, P. D., "An Integral Prediction Method for Three-Dimensional Compressible Turbulent Boundary Layers," RAE R&M 3739, Dec. 1972.

[14]Stock, H. W., "Integral Method for the Calculation of Three-Dimensional Laminar and Turbulent Boundary Layers," NASA TM 75320, July 1978.

[15]Cumpsty, N. A. and Head, M. R., "The Calculation of Three-Dimensional Turbulent Boundary Layers. Part 1: Flow over the Rear of an Infinite Swept Wing," *The Aeronautical Quarterly*, Vol. 18, 1967, pp. 55-84.

[16]Cebeci, T., Kaups, K., and Ramsey, J. A., "A General Method for Calculating Three-Dimensional Compressible Laminar and Turbulent Boundary Layers on Arbitrary Wings," NASA CR-2777, 1977.

[17]Tassa, A., Atta, E. H., and Lemmerman, L. A., "A New Three-Dimensional Boundary Layer Calculation Method," AIAA Paper 82-0224, Jan. 1982.

[18]Swaffard, T. W., "Calculation of Skin Friction in Two-Dimensional, Transonic Turbulent Flow," AEDC-TR-79-12 (AD-A0607423), April 1979.

[19]White, F. M., *Viscous Fluid Flow*, McGraw-Hill Book Co., New York, 1974, pp. 516-517, 532.

[20]Whitfield, D. L., "Integral Solution of Compressible Turbulent Boundary Layer Using Improved Velocity Profiles," AEDC-TR-78-42 (AD-A062946), Dec. 1978.

[21]Humphreys, D. A., "Comparison of Boundary Layer Calculations for a Wing: The May 1978 Stockholm Workshop Test Case," FFA TN AE-1522, Jan. 1979.

[22]Lindhout, J. P. F., van den Berg, B., and Elsenaar, A., "Comparison of Boundary Layer Calculations for the Root Section of a Wing—The September 1979 Amsterdam Workshop Test Case," NLR MP 80028 U, March 1981.

[23]Wang, K. C., "On the Determination of the Zones of Influence and Dependence for Three-Dimensional Boundary Layer Equations," *Journal of Fluid Mechanics*, Vol. 48, Pt. 2, 1972, pp. 297-404.

[24]Whitfield, D. L., Swafford, T. W., and Jacocks, J. L., "Calculation of Turbulent Boundary Layers with Separation and Viscous-Inviscid Interaction," *AIAA Journal*, Vol. 19, Oct. 1981, pp. 1315-1322.

[25]Johnston, J. P., "Three-Dimensional Turbulent Boundary Layers," M.I.T. Gas Turbine Lab., Cambridge, Mass., Rept. 39, 1957.

[26]Swafford, T. W., "Three-Dimensional, Time-Dependent, Compressible, Turbulent, Integral Boundary-Layer Equations in General Curvilinear Coordinates and Their Numerical Solution," Ph.D. Dissertation, Mississippi State University, Mississippi State, Miss., Aug. 1983.

[27]Hirschel, E. H. and Kordulla, W., "Shear Flow in Surface-Oriented Coordinates," *Notes on Numerical Fluid Mechanics*, Vol. 4, Vieweg, 1981, pp. 10-25, 199-209.

[28]Nash, J. F. and Patel, V. C., "Three-Dimensional Turbulent Boundary Layers," *SBC Technical Books*, Atlanta, Ga., 1972, pp. 21-28.

[29]Whitfield, D. L., "Analytical Description of the Complete Two-Dimensional Turbulent Boundary-Layer Velocity Profile," AEDC-TR-77-79 (AD-A045033); also, AIAA Paper 78-1158, July 1978.

[30]Whitfield, D. L. and High, M. D., "Velocity-Temperature Relations in Turbulent Boundary Layers with Nonunity Prandtl Numbers, *AIAA Journal*, Vol. 15, March 1977, pp. 431-434.

[31]Donegan, T. L., Private communication, Calspan Field Services, Inc., Arnold AFS, Tenn., Aug. 1982.

[32]Whitfield, D. L., Swafford, T. W., and Donegan, T. L., "An Inverse Integral Computational Method for Compressible Turbulent Boundary Layers," *Recent Contributions to Fluid Mechanics*, edited by W. Haase, Springer-Verlag, 1982, pp. 294-302.

[33]Swafford, T. W., "Analytical Approximation of Two-Dimensional Separated Turbulent Boundary-Layer Velocity Profiles," *AIAA Journal*, Vol. 21, June 1983, pp. 1145-1147.

[34]Thomas, J. L., "Viscous-Inviscid Interaction Using Euler and Inverse Boundary-Layer Equations," Ph.D. Dissertation, Mississippi State University, Mississippi State, Miss., 1983.

[35]Jameson, A., Schmidt, W., and Turkel, E., "Numerical Solutions of the Euler Equations by Finite Volume Methods Using Runge-Kutta Time-Stepping Schemes," AIAA Paper 81-1259, June 1981.

[36]Lambert, J. D., *Computational Methods in Ordinary Differential Equations*, John Wiley & Sons, New York, 1979, pp. 114-123.

[37]Steger, J. L. and Warming, R. F., "Flux Vector Splitting of the Inviscid Gasdynamic Equations with Applications to Finite Difference Methods," NASA TM 78605, July 1979.

[38]Smith, P. D. and Gaffney, P. L., "Approximation of the Surface Metric Tensor by Means of Bicubic Spline Interpolation," RAE-TR-72185, Dec. 1972.

[39]van den Berg, B. and Elsenaar, A., "Measurements in a Three-Dimensional Incompressible Turbulent Boundary Layer in an Adverse Pressure Gradient Under Infinite Swept Wing Conditions," NLR TR 72092 U, 1972.

[40]Swafford, T. W. and Whitfield, D. L., "Numerical Solutions of Three-Dimensional Time-Dependent Compressible Turbulent Integral Boundary-Layer Equations in General Curvilinear Coordinates," AIAA Paper 83-1674, July 1983.

[41]Cebeci, T. and Chang, K. C., "On the Turbulence Modeling Requirements of Three-Dimensional Boundary-Layer Flow," *Recent Contributions to Fluid Mechanics*, edited by W. Haase, Springer-Verlag, 1982, pp. 31-39.